

Cryoprotective activity of Arabidopsis KS-type dehydrin depends on the hydrophobic amino acids of two active segments

メタデータ	言語: eng 出版者: 公開日: 2020-07-29 キーワード (Ja): キーワード (En): 作成者: Yokoyama, Tomoka, Ohkubo, Tomohiro, Kamiya, Keita, Hara, Masakazu メールアドレス: 所属:
URL	http://hdl.handle.net/10297/00027565

1 **ORIGINAL PAPER**

2

3 **Title**

4 Cryoprotective activity of *Arabidopsis* KS-type dehydrin depends on the hydrophobic amino acids of
5 two active segments.

6

7 **Authors**

8 Tomoka Yokoyama, Tomohiro Ohkubo, Keita Kamiya, Masakazu Hara*

9

10 Research Institute of Green Science and Technology,

11 Shizuoka University,

12 836 Ohya, Shizuoka, Shizuoka 422-8529, Japan

13

14 ***Name and address for editorial correspondence**

15 Masakazu Hara

16 Research Institute of Green Science and Technology,

17 Shizuoka University,

18 836 Ohya, Shizuoka 422-8529, Japan

19 Tel: +81-54-238-5134

20 Fax: +81-54-238-5134

21 E-mail: hara.masakazu@shizuoka.ac.jp

22

23

24

25 **Abstract**

26 Dehydrins are intrinsically disordered proteins which are related to cold tolerance in plants.
27 Dehydrins show potent cryoprotective activities for freeze-sensitive enzymes such as lactate
28 dehydrogenase (LDH). Previous studies demonstrated that K-segments conserved in dehydrins had
29 cryoprotective activities and that K-segment activities depended on the hydrophobic amino acids in
30 the segment. However, the cryoprotective roles of hydrophobic amino acids in dehydrin itself have
31 not been reported. Here, we demonstrated that hydrophobic amino acids were required for the
32 cryoprotective activity of *Arabidopsis* dehydrin AtHIRD11. Cryoprotective activities were compared
33 between AtHIRD11 and the corresponding mutant in which all hydrophobic residues were changed
34 to T (AtHIRD11 Φ /T) by using LDH. The change strikingly reduced AtHIRD11 activity. A
35 segmentation analysis indicated that the conserved K-segment (Kseg) and a previously unidentified
36 segment (non-K-segment 1, NK1) showed cryoprotective activities. Circular dichroism indicated
37 that the secondary structures of all peptides showed disorder, but only cryoprotective peptides
38 changed to the ordered forms by sodium dodecyl sulfate. Ultracentrifuge analysis indicated that
39 AtHIRD11 and AtHIRD11 Φ /T had similar molecular sizes in solution. These results suggest that not
40 only structural disorder but also hydrophobic amino acids contributed to the cryoprotective activity
41 of AtHIRD11. A possible mechanism based on an extended molecular shield model is proposed.

42

43 **Keywords** Cold stress; Cryoprotection; Dehydrin; Hydrophobicity; Intrinsically disordered proteins;
44 Late embryogenesis abundant (LEA) proteins

45

46

47 **1. Introduction**

48

49 Dehydrins are group 2 late embryogenesis abundant (LEA) proteins involved in environmental
50 stress responses in plants [1, 2]. The expression responded to diverse stresses such as cold, drought,
51 high salinity, and pathogen infection [3-5]. Although some groups of LEA proteins have been found
52 in kingdoms other than plants, dehydrins are likely plant-specific [6]. Since dehydrins ubiquitously
53 accumulate in various tissues and organelles such as cytoplasm, nucleus, plastid, mitochondrion,
54 endoplasmic reticulum, and plasma membrane [3, 6], dehydrin has been proposed to play
55 fundamental roles in the protection of cellular components. Data from circular dichroism (CD),
56 Fourier-transform infrared spectroscopy (FTIR), and nuclear magnetic resonance (NMR) have
57 shown that dehydrins are intrinsically disordered proteins [7-10]. The intrinsic disorder of dehydrins
58 is thought to be due to a high abundance of hydrophilic amino acids [5].

59 Dehydrins are identified by the presence of K-segments (typical sequence:
60 EKKGIMEKIKEKLPG). Y-segments (e.g., DEYGNP) and S-segments (e.g.,
61 LHRSGSSSSSEDD) are other conserved sequences, although they are not found in all dehydrins
62 [5, 6]. Dehydrin types have been classified using the letters K, Y, and S [11]. In addition to these
63 segments, Φ -segments (G- and polar amino acid-rich sequences) [11], F-segments
64 (DRGLFDLGGK) [12, 13], and ChP-segments [5] have been described. Extensive studies have
65 elucidated the functions of these segments. K-segments protected freeze-sensitive enzymes such as
66 lactate dehydrogenase (LDH, EC 1.1.1.27) [14, 15] and bound to phospholipids while maintaining
67 membrane fluidity at low temperature [10, 16, 17]. S-segments bound to Ca^{2+} after phosphorylation
68 [18]. Φ -Segments might be related to the intrinsically disordered nature of dehydrins, because the
69 segments were rich in Gs and polar amino acids [19]. F-segments had cryoprotective activities for
70 LDH [20]. K-rich regions including the ChP-segments were involved in DNA binding [21, 22].
71 H-rich sequences frequently found in dehydrins bound to transition metals [23], reduced the
72 generation of reactive oxygen species [24], and controlled membrane binding [17].

73 Although various stresses cause the gene expression of dehydrins, cold is a major cue for dehydrin
74 accumulation in plants [5]. Transgenic plants expressing dehydrin genes were more cold tolerant
75 than the corresponding wild-type plants (e.g., [25-30]), suggesting that dehydrins might prevent
76 cellular damage due to cold. The in vitro functions of dehydrins under cold stress have also been
77 investigated. Cryoprotective activities for cold-sensitive enzymes (e.g., [31-34]), membrane bindings
78 (e.g., [10, 16, 17, 35]), and defense against ROS (e.g., [22, 24]) have been found. Accordingly,
79 dehydrins have been thought to be multifunctional (moonlighting) proteins [36, 37].

80 Recently, intensive studies have elucidated the cryoprotective mechanism of dehydrins. The
81 molecular sizes of dehydrins were the primary factors in the cryoprotective activities of dehydrins,
82 i.e., larger dehydrins exhibited greater cryoprotective activities [14]. This finding was fit to the
83 molecular shield model, which can generally explain how peptides protect proteins [38]. Besides that,
84 studies of cryoprotective mechanisms have focused on the specific sites of dehydrin sequences.
85 Truncation of K-segments from dehydrins (ERD10, RcDhn5, TaDHN-5, and WZY2) reduced the
86 dehydrins' full cryoprotective activities [34, 39, 40]. K-segments and F-segments had cryoprotective
87 activities [14, 15, 20]. Intriguingly, when the hydrophobic amino acids of K- and F-segments were
88 changed to polar uncharged T residues, the activities of the segments were remarkably reduced,
89 suggesting that the hydrophobic residues were crucial for the cryoprotective activities of K- and
90 F-segments [15, 20]. This implies that not only the segments but also the dehydrin itself may require
91 hydrophobic amino acids for cryoprotective activities. However, no study has investigated this issue.

92 In order to confirm the roles of hydrophobic amino acids in dehydrin, we used AtHIRD11
93 (At1g54410), the SK-type dehydrin of *Arabidopsis thaliana* [41]. This dehydrin is short (98 amino
94 acids) with a simple segment composition (one K-segment and one S-segment). Previous
95 investigations of AtHIRD11 showed diverse molecular functions: cryoprotective activity [42],
96 inhibition of ROS generation [24], and recovery of metal-inhibited enzyme activity [43]. Here we

97 prepared AtHIRD11 and the mutant protein designated as AtHIRD11 Φ /T, in which all 11
98 hydrophobic residues of AtHIRD11 were changed to T. This change greatly reduced the
99 cryoprotective activity of AtHIRD11. We also found a previously unidentified segment whose
100 cryoprotective activity was as potent as that of the K-segment of AtHIRD11. Finally, on the basis of
101 the molecular shield model, we propose an additional mechanism regarding the cryoprotective
102 activities of dehydrins.

103

104

105 **2. Materials and methods**

106

107 *2.1. Chemicals and peptides*

108

109 Sodium dodecyl sulfate (SDS), sodium pyruvate, and 8-anilino-1-naphthalene sulfonic acid (ANS)
110 were purchased from Sigma (Tokyo, Japan). Nicotine adenine dinucleotide (NADH) and
111 recombinant lactate dehydrogenase (LDH) from rabbit muscle were obtained from Oriental Yeast
112 (Tokyo, Japan). AtHIRD11 and AtHIRD11 Φ /T were prepared by the
113 9-fluorenylmethoxycarbonyl-based long-peptide synthetic system of Biosynthesis Inc. (Lewisville,
114 TX, USA). N-terminal FITC-labeled AtHIRD11 (i.e., FITC-AtHIRD11) and AtHIRD11 Φ /T (i.e.,
115 FITC-AtHIRD11 Φ /T) were prepared by the same system. The alkyl spacer of aminohexanoic acid
116 was used. After removing impurities, the peptides were identified by a Voyager DE-RP mass
117 spectrometer (Applied Biosystems, Foster City, CA, USA). The segments (i.e., NK1-6 and Kseg)
118 were synthesized with the automated apparatus by using the solid-phase method (Tetras, Advanced
119 ChemTech, Louisville, KY, USA). Each peptide was purified by reversed-phase chromatography
120 (UFLC-20AB, Shimadzu, Kyoto, Japan) with an Alltima C18 column (4.6 x 250 mm, Alltech

121 Associates, Deerfield, IL, USA). A linear gradient of acetonitrile from 5% to 95% in 0.05%
122 trifluoroacetic acid solution was performed over 25 min. Mass spectrometry (LCMS-2020,
123 Shimadzu) was used for identification. The proteins and peptides were stored at -20°C after
124 lyophilization. In the following experiments, peptide concentrations were calculated from the gross
125 weight of lyophilized powder. Purities determined by HPLC were used for the calculation.

126

127 *2.2. Sodium dodecyl sulfate-polyacrylamide gel electrophoresis (SDS-PAGE)*

128

129 AtHIRD11, AtHIRD11Φ/T, FITC-AtHIRD11, and FITC-AtHIRD11Φ/T were analyzed by
130 SDS-PAGE (12% polyacrylamide gel) with molecular weight markers (Kaleidoscope markers,
131 Bio-Rad, Tokyo, Japan). AtHIRD11 and AtHIRD11Φ/T were stained with Coomassie Blue (BioSafe,
132 Bio-Rad). FITC-AtHIRD11 and FITC-AtHIRD11Φ/T were detected by a fluorescence imaging
133 system (Fusion FX, Vilber-Lourmat, Marne-la-Vallée, France).

134

135 *2.3. Cryoprotective assays for LDH*

136

137 Cryoinactivation, cryodenaturation, and cryoaggregation were inhibited to evaluate the
138 cryoprotective activities of peptides by using LDH. The procedures were according to a previous
139 method [15] with modifications (Supplementary Fig. 1).

140 Inhibition of cryoinactivation was measured as follows. In 1.5-mL plastic tubes, AtHIRD11 and
141 AtHIRD11Φ/T solutions (30 μL) at concentrations of 0, 0.0017, 0.017, 0.17, 0.83, 1.7, 3.3, 8.3, 17,
142 and 100 μM in 10 mM Tris-HCl buffer pH 7.5 were combined with the LDH solution (20 μL, 0.34
143 μM as a monomer) in the same buffer. In this step, the final concentrations of AtHIRD11 and
144 AtHIRD11Φ/T were 0, 0.001, 0.01, 0.1, 0.5, 1, 2, 5, 10, and 60 μM, respectively. The final

145 concentration of LDH as a monomer was 0.14 μM . The tubes were treated with a freezing and
146 thawing process (in liquid N_2 for 1 min and then in a water bath at $25\pm 2^\circ\text{C}$ for 3 min). This
147 freezing-thawing cycle was repeated in triplicate. To measure the LDH activities, the samples treated
148 with the freezing-thawing cycles (4 μL) were combined with reaction solutions (196 μL , 9.5 mM
149 Tris-HCl pH 7.5, 0.58 mM sodium pyruvate, and 60 μM NADH) in a 96-well microplate.
150 Absorbance at 340 nm was monitored with a microplate reader (Varioskan Flash, Thermo Fisher
151 Scientific, Tokyo, Japan) at 25 $^\circ\text{C}$. The three freezing-thawing cycles reduced LDH activity to 15 to
152 20% of the initial level. After measuring the LDH activities before and after the freezing-thawing
153 cycles, the relative cryoinactivation of LDH (%) was determined. One-hundred percent relative
154 cryoinactivation means a decreased degree of LDH activity by the freezing-thawing cycles without
155 peptide. The inhibition of cryoinactivation was evaluated as a 50% protection dose (PD_{50}). If the
156 relative cryoinactivation was higher than 50% even when the peptide concentrations reached 60 μM
157 (the case with AtHIRD11 Φ /T), PD_{50} was represented as more than 60 μM . When segments (NK1-6
158 and Kseg) were used, the experimental conditions were the same as above with the following
159 exception: the peptide concentrations were 0, 0.033, 0.33, 3.3, 8.3, 17, 33, 83, 170, and 500 μM ,
160 respectively.

161 Inhibition of cryodenaturation was determined by using ANS, which is a fluorescence probe for
162 hydrophobicity on the protein surface. ANS (10 μM), LDH (4 μM), and dehydrins (AtHIRD11 and
163 AtHIRD11 Φ /T) (0, 0.001, 0.01, 0.1, 1, 2, 5, 10, 20, and 35 μM) were combined in 10 mM sodium
164 phosphate buffer pH 7.0 in a total volume of 250 μL in 1.5-ml plastic tubes. For the segments
165 (NK1-6 and Kseg), different series of concentrations (0, 2, 5, 10, 20, 60, 100, and 300 μM) were
166 used. The three freezing-thawing cycles were performed as described above. The samples were taken
167 in the 96-well plates followed by fluorescence detection (Ex 350 nm and Em 470 nm, Varioskan
168 Flash). The increment of fluorescence promoted by the freezing-thawing treatment in the sample

169 containing no dehydrin (or segment) was standardized as 100%. The inhibition of cryodenaturation
170 was represented as the PD₅₀. If the relative increment of fluorescence was higher than 50% even
171 when the concentrations of dehydrins and segments reached 35 μM and 300 μM, respectively, PD₅₀
172 was designated as more than 35 μM (dehydrins) or 300 μM (segments).

173 For the inhibition of cryoaggregation, sample solutions (250 μL) containing LDH (4 μM) and
174 dehydrins (AtHIRD11 and AtHIRD11Φ/T) (0, 0.001, 0.01, 0.1, 1, 2, 5, 10, 20, and 35 μM) were
175 prepared. The concentrations of segments (NK1-6 and Kseg) were 0, 2, 5, 10, 20, 60, 100, and 300
176 μM, respectively. After the three freezing-thawing cycles, 200 μL of each sample was subjected to a
177 96-well microplate assay (415 nm, Bio-Rad iMark). A turbidity increment induced by the
178 freezing-thawing treatment in the sample without dehydrin (or segment) was standardized as 100%.
179 The PD₅₀ was used to show the inhibition of cryoaggregation. When the relative increment of
180 turbidity was higher than 50% at all concentrations of dehydrins and segments, PD₅₀ was designated
181 as more than 35 μM (dehydrins) and 300 μM (segments), respectively.

182

183 *2.4. Circular dichroism (CD)*

184

185 CD was applied to analyze the secondary structures of dehydrins and segments. Dehydrins
186 (AtHIRD11 and AtHIRD11Φ/T, 4.7 μM) or segments (NK1-6 and Kseg) were mixed with SDS (0.1,
187 1, and 10 mM) in 10 mM Tris-HCl buffer pH 7.5. The samples were subjected to a
188 spectropolarimeter (J-820, Jasco, Tokyo, Japan) under the following measurement conditions: scan
189 range from 190 to 250 nm, scan speed 100 nm min⁻¹, resolution 1 nm, and cell width 2 mm. Putative
190 compositions of secondary structures were obtained by K2D3 software
191 (<http://cbdm-01.zdv.uni-mainz.de/~andrade/k2d3/>) [44].

192

193 2.5. *Structure prediction*

194

195 Disordered structures of proteins were analyzed with IUPred (<https://iupred2a.elte.hu/>) [45] and
196 DisEMBL 1.5 (<http://dis.embl.de/>) [46]. PEP-FOLD3
197 (<http://bioserv.rpbs.univ-paris-diderot.fr/services/PEP-FOLD3/>) [47] was used to predict peptide
198 structures. Models with the best TM scores in the neutral solution were chosen.

199

200 2.6. *Analytical ultracentrifugation*

201

202 To predict the molecular sizes of dehydrins in solution, sedimentation velocity experiments were
203 conducted with an Optima XL-I analytical ultracentrifuge (Beckman-Coulter, Brea, CA, USA) using
204 an eight-hole An50Ti rotor at 20 °C. Since AtHIRD11 has little absorption at the detection range of
205 the analytical ultracentrifuge, N-terminal FITC-labeled dehydrins (i.e., FITC-AtHIRD11 and
206 FITC-AtHIRD11 Φ /T) were used. FITC-dehydrins (30 μ M) were dissolved in 10 mM Tris-HCl
207 buffer (pH 7.5) containing 150 mM NaCl. The samples were centrifuged at 50,000 rpm and detected
208 at 494 nm. All data were collected without time intervals between scans. After obtaining the moving
209 boundaries and the residuals between raw and theoretically fitted data points, sedimentation
210 coefficients and molecular sizes were calculated by the $c(s)$ method in SEDFIT [48]. The
211 ultracentrifugation experiments were performed twice.

212

213 2.7. *Statistical analysis*

214

215 Data for P values were analyzed by Dunnett's test at a significance level of 0.05.

216

217

218 3. Results

219

220 3.1. Cryoprotective activity of *AtHIRD11*

221

222 In this study we used *AtHIRD11* (At1g54410), one of the 10 *Arabidopsis* dehydrins. The sequence
223 of *AtHIRD11* is shown in Fig. 1A. This dehydrin is small and consists of a simple segment
224 composition (KS-type). The *AtHIRD11* gene was abundantly expressed in *Arabidopsis*, and the
225 *AtHIRD11* protein was detected in all organs of the plant, with accumulation in the cambial zone of
226 the stem vasculature [41]. Due to such abundant pre-accumulation, the gene and protein expression
227 levels in *Arabidopsis* were only weakly enhanced by various stresses, including cold. However, the
228 *AtHIRD11* orthologues, such as *CAS15* of *Medicago sativa* [49], *Dhn13* of *Hordeum vulgare* [50],
229 and *DHN10* of *Solanum* species [51], were considerably induced.

230 A previous study reported that *AtHIRD11* showed cryoprotective activity for malate
231 dehydrogenase [42]. To test whether hydrophobic amino acids were required for the cryoprotective
232 activity of *AtHIRD11*, we used *AtHIRD11*Φ/T in which all 11 hydrophobic amino acids of
233 *AtHIRD11* were changed to polar, uncharged amino acids (Ts) (Fig. 1B). Both *AtHIRD11* and
234 *AtHIRD11*Φ/T were chemically synthesized and highly purified. SDS-PAGE detected *AtHIRD11*
235 and *AtHIRD11*Φ/T as bands at approximately 17,000 and 25,000, respectively (Fig. 1C). Since the
236 calculated molecular weights of *AtHIRD11* and *AtHIRD11*Φ/T were 10796 and 10673, respectively,
237 their migrations in SDS-PAGE were shorter than expected. Moreover, the bands were faint after the
238 Coomassie blue staining. Such unusual behaviors in SDS-PAGE have been frequently observed in
239 many dehydrins (e.g., [52]). In order to clearly detect *AtHIRD11* and *AtHIRD11*Φ/T in the gel, we
240 prepared N-terminal FITC-labeled peptides (i.e., FITC-*AtHIRD11* and FITC-*AtHIRD11*Φ/T).

241 Fluorescence imaging found apparent bands of FITC-AtHIRD11 and FITC-AtHIRD11Φ/T (Fig. 1D)
242 at the corresponding sites of AtHIRD11 and AtHIRD11Φ/T (Fig. 1C), respectively.

243 The cryoprotective activities of AtHIRD11 and AtHIRD11Φ/T for LDH were determined (Fig. 2).
244 Three items were tested: the inhibition of cryoinactivation, cryodenaturation, and cryoaggregation.
245 The PD₅₀ values were used to determine the inhibition activities. The results indicated that
246 AtHIRD11 apparently inhibited cryoinactivation, cryodenaturation, and cryoaggregation, whereas
247 AtHIRD11Φ/T did not inhibit them. This suggests that hydrophobic amino acids contributed to the
248 cryoprotective activity of AtHIRD11. Additionally, FITC-AtHIRD11 inhibited the cryoinactivation
249 of LDH at a degree similar to that of AtHIRD11, but FITC-AtHIRD11Φ/T did not inhibit it
250 (Supplementary Fig. 2). Thus, the N-terminal FITC-labeling might not influence the cryoprotective
251 activities of AtHIRD11 and AtHIRD11Φ/T.

252

253 *3.2. Cryoprotective segments of AtHIRD11*

254

255 We previously found that the K-segment of AtHIRD11 (H₄₁KEGIVDKIKDKIHG₅₅) showed
256 cryoprotective activity for LDH [15]. However, the cryoprotective activities of other segments were
257 not tested. Thus, we divided the AtHIRD11 sequence into 7 segments, each consisting of 15 amino
258 acids (Fig. 3A). AtHIRD11 had the K-segment (Kseg) in the middle of the sequence. The N-terminal
259 half region and the C-terminal half region were separated into NK1 to NK3 and NK4 to NK6,
260 respectively. Here, NK means non-K-segment. The cryoprotective activities of the seven segments
261 were determined by measuring the inhibition of cryoinactivation, cryodenaturation, and
262 cryoaggregation of LDH (Fig. 3B). Not only Kseg but also NK1 remarkably inhibited the
263 cryoinactivation of LDH. The activity of Kseg tended to be higher than that of NK1, although the
264 difference was not significant. The PD_{50s} of the other segments (i.e., NK2 to NK6) were more than

265 300 μ M, indicating that these segments hardly inhibited the cryoinactivation of LDH. Similar results
266 were obtained in the inhibition of cryodenaturation and cryoaggregation. Taken together, these
267 results suggested that NK1 and Kseg were the cryoprotective sites of AtHIRD11. Nevertheless, it
268 should be noted that AtHIRD11 itself showed more potent inhibition of cryoinactivation,
269 cryodenaturation, and cryoaggregation of LDH than did NK1 and Kseg.

270

271 *3.3. Intrinsic disorder of AtHIRD11 and AtHIRD11 Φ /T*

272

273 Since protein functions are related to the protein structures, the difference in cryoprotective
274 activities between AtHIRD11 and AtHIRD11 Φ /T was thought to be attributed to their structural
275 distinction. Thus, we investigated the secondary structures of AtHIRD11 and AtHIRD11 Φ /T. Since it
276 has been confirmed that dehydrins are intrinsically disordered proteins, we predicted the structural
277 disorder of AtHIRD11 and AtHIRD11 Φ /T by using IUPred and DisEMBL. The IUPred analysis
278 indicated that both AtHIRD11 and AtHIRD11 Φ /T were highly disordered over the whole sequences
279 (Fig. 4A). When the positions of the segments were mapped, the IUPred scores corresponding to the
280 regions of NK1 and Kseg were somewhat different: the scores in NK1 and Kseg of AtHIRD11 were
281 lower than those of AtHIRD11 Φ /T. Similar trends were observed in the DisEMBL analysis
282 (Supplementary Fig. 3). The *in silico* results were reconfirmed by CD. AtHIRD11 and
283 AtHIRD11 Φ /T showed strong negatives at around 200 nm (Fig. 4B, gray broken lines, arrowheads),
284 which are typical signals for disorder. According to the K2D3 analysis, both proteins had low
285 compositions of α -helix and β -strand (sums were less than 15%) (Fig. 4C, 0 mM SDS), indicating
286 that AtHIRD11 and AtHIRD11 Φ /T were highly disordered in solution.

287 It has been repeatedly reported that secondary structures of dehydrins were transferred from
288 disorder to order by the addition of SDS (many papers, e.g., [16, 53]). Although it was demonstrated

289 that dehydrins bound to SDS mainly by electrostatic force [54, 55], the driving factors in the
290 SDS-induced structural transition have not been fully confirmed. Here we conducted the CD analysis
291 to test whether SDS affected the secondary structures of AtHIRD11 and AtHIRD11 Φ /T. As expected,
292 SDS (1 and 10 mM) altered the AtHIRD11 structure from disordered to ordered. On the contrary,
293 little change was detected in AtHIRD11 Φ /T even at 10 mM of SDS (Fig. 4B, C). Subsequently, we
294 corrected the CD data for the seven segments (i.e., NK1 to NK6, and Kseg). All the segments were
295 in disordered states under the condition without SDS (Fig. 5A, gray broken lines, arrowheads).
296 When SDS was added, only NK1 and Kseg showed significant increases in the α -helix and β -strand
297 compositions (Fig. 5B). In the other segments, however, SDS caused slight or no structural changes.
298 The results suggested that the SDS-induced structural transition of AtHIRD11 depended on the
299 hydrophobic amino acids and was related to the structural changes in NK1 and Kseg.

300

301 3.4. Sizes of AtHIRD11 and AtHIRD11 Φ /T molecules in solution

302

303 The molecular sizes of AtHIRD11 and AtHIRD11 Φ /T in aqueous solution were determined by the
304 sedimentation coefficients obtained by analytical ultracentrifugation. The averages of molecular
305 weights obtained from the experiments conducted twice were 14,100 (AtHIRD11) and 14,000
306 (AtHIRD11 Φ /T) (Table 1). Because the calculated molecular weights were 11298
307 (FITC-AtHIRD11) and 11236 (FITC-AtHIRD11 Φ /T), both peptides were monomeric in the solution.
308 The data seemed contradictory to the previous results that dehydrins from *Opuntia streptacantha* and
309 *Arabidopsis thaliana* showed the dehydrin-dehydrin interaction in vivo [56, 57]. This might be
310 attributable to the difference in dehydrin types: AtHIRD11 is the KS-type but the dehydrins used in
311 the previous studies were SKn- and YnSKn-types. Eventually, the molecular sizes in solution were
312 not much different between AtHIRD11 and AtHIRD11 Φ /T. Therefore, the reduction of AtHIRD11's

313 cryoprotective activity was not due to the alteration of molecular size by changing the hydrophobic
314 amino acids to Ts

315

316

317 **4. Discussion**

318

319 The present results demonstrated that the hydrophobic residues were required for the
320 cryoprotective activity of AtHIRD11, which is the *Arabidopsis* KS-type dehydrin. We also found
321 that two segments of AtHIRD11 (NK1 and Kseg) showed cryoprotective activities, but other
322 segments did not (Fig. 3B). Although the K-segment has been well documented as the conserved
323 sequence of dehydrins, the NK1 sequence has not been studied yet. According to a protein BLAST
324 search (<https://blast.ncbi.nlm.nih.gov/Blast.cgi>), KS-type dehydrins were found in angiosperms, but
325 not in gymnosperms, moss, or cyanobacteria. This suggested that the KS-type dehydrin genes were
326 generated in angiosperms after the separation of gymnosperms and angiosperms. The multiple
327 alignment analysis showed that not only Kseg but also NK1 were conserved in the KS-type dehydrin
328 orthologues (Supplementary Fig. 4). Considering that only NK1 and Kseg had efficient
329 cryoprotective activities, it was supposed that during the evolution of KS-type dehydrins, both
330 segments were maintained as functional domains.

331 Here, we discuss the cryoprotective mechanisms of NK1 and Kseg. Without reference to the
332 cryoprotective activities, all segments (i.e., NK1-6 and Kseg) showed disordered structures in
333 aqueous solution (Fig. 5). However, it is noteworthy that only the cryoprotective segments (i.e., NK1
334 and Kseg) had multiple hydrophobic amino acids and changed their structures from disordered to
335 ordered by SDS. When NK1 and Kseg sequences were analyzed by HeliQuest software
336 (<https://heliquet.ipmc.cnrs.fr/>) [58], the hydrophobic amino acids were gathered on one side of each

337 wheel, whereas the charged amino acids were located on the opposite side (Supplementary Fig. 5).
338 This suggests that SDS induced amphipathic helices in the structures of NK1 and Kseg. Similarly,
339 the PEP-FOLD3 software predicted that NK1 and Kseg might have elongated hydrophobic areas on
340 one side of the surface of each peptide (Supplementary Fig. 6). However, it should be noted that the
341 prediction tools could show one of the possible structures of the disordered peptides, and the
342 disorder-to-order transitions by SDS seemed artificial because the SDS concentrations were
343 considerably high. Nevertheless, it is undeniable that NK1 and Kseg might be in equilibrium
344 between disorder and order in solution, whereas disorder was excessively abundant. If so, the
345 transient formation of amphipathic structures may be required for the cryoprotective activities of
346 NK1 and Kseg. Putative correlations between the formation of hydrophobic areas and the expression
347 of cryoprotective activities were found also in a typical K-segment [15] and F-segments [20].
348 Moreover, the enzyme-protective region of *Arabidopsis* group 4 LEA protein (AtLEA4-5)
349 transiently formed an amphipathic helix [59]. Taken together, the present and previous results
350 indicate it is likely that the transient amphipathic structures are crucial for the activities of
351 cryoprotective segments of LEA proteins.

352 As shown in Fig. 2, hydrophobic residues were required for the cryoprotective activity of
353 AtHIRD11. In addition, most hydrophobic residues of AtHIRD11 were localized in NK1 and Kseg,
354 which were the only segments that showed cryoprotective activities (Fig. 3). This implies that NK1
355 and Kseg were specific sites for the cryoprotective activities of AtHIRD11. However, since the
356 cryoprotective activity of AtHIRD11 was remarkably higher than those of NK1 and Kseg (Fig. 3B),
357 AtHIRD11's activity did not depend merely on the activities of the two segments. The size effect due
358 to the intrinsic disorder of AtHIRD11 seems to be related to the potent cryoprotective activity. This
359 is consistent with the previous data showing that size and disorder are important for the
360 cryoprotective effects of dehydrins [14].

361 The SDS-PAGE analysis indicated that the migration of AtHIRD11 was much larger than that of
362 AtHIRD11 Φ /T, indicating that AtHIRD11 was likely more compact than AtHIRD11 Φ /T under the
363 SDS-PAGE conditions, because SDS promoted the structural change from disordered to ordered in
364 AtHIRD11 but not in AtHIRD11 Φ /T (Fig. 4B, C). Indeed, the SDS concentration in SDS-PAGE was
365 approximately 3.5 mM, a concentration that could induce the disorder-to-order transition of
366 AtHIRD11 but not that of AtHIRD11 Φ /T. This observation might suggest that, although both
367 AtHIRD11 and AtHIRD11 Φ /T were flexible in solution, only AtHIRD11 could increase the
368 frequency of an ordered structure in the local hydrophobic environment. This structural alteration
369 might be concomitant with the formation of amphipathic structures of NK1 and Kseg. Meanwhile, it
370 should be acknowledged that AtHIRD11 was still rather flexible in SDS-PAGE because the size of
371 AtHIRD11 was approximately 17,000, whereas the calculated molecular weight of AtHIRD11 was
372 10796. It cannot be denied that AtHIRD11 migrated larger than AtHIRD11 Φ /T in SDS-PAGE
373 because AtHIRD11 could bind more SDS molecules than AtHIRD11 Φ /T. In this case, the difference
374 of molecular sizes between AtHIRD11 and AtHIRD11 Φ /T cannot be determined from the results of
375 SDS-PAGE.

376 It has been discussed whether dehydrins access target proteins during cryoprotection. NMR
377 analysis indicated that the *Vitis* dehydrin did not bind to LDH [33]. Using analytical
378 ultracentrifugation, we also confirmed that FITC-AtHIRD11 did not bind to LDH (Supplementary
379 Fig. 7). It was noted that the minimum complementary area required to make a water-tight seal
380 between interacting proteins was estimated to be at least 600 Å² [60]. If dehydrins reach the
381 hydrophobic area of LDH, they may not bind tightly to LDH, because the contact surface between
382 dehydrins and LDH is not large enough.

383 Finally, we predict the cryoprotective mechanism of AtHIRD11 based on the present data
384 combined with previous knowledge. In solution, AtHIRD11 was highly flexible but may have

385 infrequently taken a partially ordered structure. The transient ordering might be associated with the
386 formation of amphipathic structures of NK1 and Kseg. At the same time, the partially ordered form
387 may transiently interact with the hydrophobic patches on the surface of the cold-stressed LDH [61].
388 The hydrophobic patches can also be generated at the connecting sites between monomers, because
389 LDH is a tetrameric protein (Supplementary Fig. 7) [61]. After that, LDH was restored and
390 AtHIRD11 was returned to the flexible form (an entropy transfer). During this process, the
391 disordered region of AtHIRD11, which was still flexible, may have prevented the collision between
392 LDH molecules.

393 At this time, several models have been proposed to explain the actions of protective peptides. In
394 the basic molecular shield model [38], peptides may occupy the space to prevent target proteins from
395 colliding without binding to the proteins. An extended molecular shield model (or an entropy
396 transfer model) shows that protective peptides may cover and restore the misfolded proteins by
397 loosely associating the peptides to the target proteins [62]. An interaction model was also supposed
398 in which the peptides may protect the proteins by the protein-protein interaction [63]. Considering
399 that the transient hydrophobic interaction may be crucial for AtHIRD11's cryoprotective activity, its
400 cryoprotective mechanism is thought to fit the extended molecular shield model, whereas other
401 models can partially explain our results. On the other hand, inactive AtHIRD11 Φ /T, which had no
402 hydrophobic amino acid, may not have taken an ordered structure. Thus, it is likely that
403 AtHIRD11 Φ /T failed to interact with the hydrophobic patches of LDH and could not perform the
404 entropy transfer.

405

406

407 **5. Conclusion**

408

409 AtHIRD11 showed cryoprotective activities for LDH in a hydrophobic residue-dependent manner.
410 NK1 and Kseg, both of which contained hydrophobic amino acids, contributed to the cryoprotective
411 activity. The hydrophobic residues of AtHIRD11 are related not only to the interaction between the
412 dehydrins and the hydrophobic patches of LDH but also to the transient change in AtHIRD11
413 between flexible and ordered forms. The transient change is likely crucial for dehydrin's
414 cryoprotective activity. This work revealed that, although dehydrins are intrinsically disordered
415 proteins with low contents of hydrophobic amino acids, the hydrophobic residues can play important
416 roles in the cryoprotective activities of dehydrins.

417

418

419 **Acknowledgements**

420

421 This study was supported by Grant-in-Aids (18H02222 and 19K22274) for Scientific Research
422 from the Ministry of Education, Culture, Sports, Science, and Technology of Japan.

423

424 **Declaration of competing interest**

425

426 All the authors declare no conflict of interest.

427

428

429 **References**

430 [1] M. Hundertmark, D.K. Hincha, LEA (late embryogenesis abundant) proteins and their encoding
431 genes in *Arabidopsis thaliana*, BMC Genom. 9 (2008) 118.

432

- 433 [2] S.C. Hand, M.A. Menze, M. Toner, L. Boswell, D. Moore, LEA proteins during water stress: not
434 just for plants anymore, *Annu. Rev. Physiol.* 73 (2011) 115-134.
435
- 436 [3] S.K. Eriksson, P. Harryson, Dehydrins: molecular biology, structure and function, in: U. Lüttge,
437 E. Beck, D. Bartels (Eds.), *Plant desiccation tolerance, Ecological studies (analysis and synthesis)*,
438 vol 215, Springer, Berlin, Heidelberg, 2011, pp. 289-305.
439
- 440 [4] M. Hanin, F. Brini, C. Ebel, Y. Toda, S. Takeda, Plant dehydrins and stress tolerance: versatile
441 proteins for complex mechanisms, *Plant Signal. Behav.* 6 (2011) 1503-1509.
442
- 443 [5] S.P. Graether, K.F. Boddington, Disorder and function: a review of the dehydrin protein family,
444 *Front. Plant Sci.* 5 (2014) 576.
445
- 446 [6] A. Tunnacliffe, M.J. Wise, The continuing conundrum of the LEA proteins. *Naturwissenschaften*
447 94 (2007) 791-812.
448
- 449 [7] E.E. Findlater, S.P. Graether, NMR assignments of the intrinsically disordered K 2 and YSK 2
450 dehydrins, *Biomol. NMR Assign.* 3 (2009) 273-275.
451
- 452 [8] L.N. Rahman, G.S. Smith, V.V. Bamm, J.A. Voyer-Grant, B.A. Moffatt, J.R. Dutcher, G. Harauz,
453 Phosphorylation of *Thellungiella salsuginea* dehydrins TsDHN-1 and TsDHN-2 facilitates
454 cation-induced conformational changes and actin assembly, *Biochemistry* 50 (2011) 9587-9604.
455
- 456 [9] B.S. Ágoston, D. Kovács, P. Tompa, A. Perczel, Full backbone assignment and dynamics of the

457 intrinsically disordered dehydrin ERD14, *Biomol. NMR Assign.* 5 (2011) 189-193.
458

459 [10] M.W. Clarke, K.F. Boddington, J.M. Warnica, J. Atkinson, S. McKenna, J. Madge, C.H. Barker,
460 S.P. Graether, Structural and functional insights into the cryoprotection of membranes by the
461 intrinsically disordered dehydrins, *J. Biol. Chem.* 290 (2015) 26900-26913.
462

463 [11] T.J. Close, Dehydrins: a commonality in the response of plants to dehydration and low
464 temperature, *Physiol. Plant.* 100 (1997) 291-296.
465

466 [12] G.R. Strimbeck, Hiding in plain sight: the F segment and other conserved features of seed plant
467 SKn dehydrins, *Planta* 245 (2017) 1061-1066.
468

469 [13] H. Wei, Y. Yang, M.E. Himmel, M.P. Tucker, S.Y. Ding, S. Yang, R. Arora, Identification and
470 characterization of five cold stress-related rhododendron dehydrin genes: spotlight on a FSK-type
471 dehydrin with multiple F-segments, *Front. Bioeng. Biotech.* 7 (2019) 30.
472

473 [14] S.L. Hughes, V. Schart, J. Malcolmson, K.A. Hogarth, D.M. Martynowicz, E. Tralman-Baker,
474 S.N. Patel, S.P. Graether, The importance of size and disorder in the cryoprotective effects of
475 dehydrins, *Plant Physiol.* 163 (2013) 1376-1386.
476

477 [15] M. Hara, T. Endo, K. Kamiya, A. Kameyama, The role of hydrophobic amino acids of
478 K-segments in the cryoprotection of lactate dehydrogenase by dehydrins, *J. Plant Physiol.* 210
479 (2017) 18-23.
480

481 [16] M.C. Koag, S. Wilkens, R.D. Fenton, J. Resnik, E. Vo, T.J. Close, The K-segment of maize
482 DHN1 mediates binding to anionic phospholipid vesicles and concomitant structural changes, *Plant*
483 *Physiol.* 150 (2009) 1503-1514.
484

485 [17] S.K. Eriksson, M. Kutzer, J. Procek, G. Gröbner, P. Harryson, Tunable membrane binding of the
486 intrinsically disordered dehydrin Lti30, a cold-induced plant stress protein, *Plant Cell* 23 (2011)
487 2391-2404.
488

489 [18] M.K. Alsheikh, B.J. Heyen, S.K. Randall, Ion binding properties of the dehydrin ERD14 are
490 dependent upon phosphorylation, *J. Biol. Chem.* 278 (2003) 40882-40889.
491

492 [19] J. Atkinson, M.W. Clarke, J.M. Warnica, K.F. Boddington, S.P. Graether, Structure of an
493 intrinsically disordered stress protein alone and bound to a membrane surface, *Biophys. J.* 111
494 (2016) 480-491.
495

496 [20] T. Ohkubo, A. Kameyama, K. Kamiya, M. Kondo, M. Hara, F-segments of *Arabidopsis*
497 dehydrins show cryoprotective activities for lactate dehydrogenase depending on the hydrophobic
498 residues, *Phytochemistry* 173 (2020) 112300.
499

500 [21] M. Hara, Y. Shinoda, Y. Tanaka, T. Kuboi, DNA binding of citrus dehydrin promoted by zinc
501 ion, *Plant Cell Environ.* 32 (2009) 532-541.
502

503 [22] K.F. Boddington, S.P. Graether, Binding of a *Vitis riparia* Dehydrin to DNA, *Plant Sci.* (2019)
504 110172.

505

506 [23] M. Hara, M. Fujinaga, T. Kuboi, Metal binding by citrus dehydrin with histidine-rich domains, J.
507 Exp. Bot. 56 (2005) 2695-2703.

508

509 [24] M. Hara, M. Kondo, T. Kato, A KS-type dehydrin and its related domains reduce Cu-promoted
510 radical generation and the histidine residues contribute to the radical-reducing activities, J. Exp. Bot.
511 64 (2013) 1615-1624.

512

513 [25] M. Hara, S. Terashima, T. Fukaya, T. Kuboi, Enhancement of cold tolerance and inhibition of
514 lipid peroxidation by citrus dehydrin in transgenic tobacco, Planta 217 (2003) 290-298.

515

516 [26] T. Puhakainen, M.W. Hess, P. Mäkelä, J. Svensson, P. Heino, E.T. Palva, Overexpression of
517 multiple dehydrin genes enhances tolerance to freezing stress in *Arabidopsis*, Plant Mol. Biol. 54
518 (2004) 743-753.

519

520 [27] X. Xing, Y. Liu, X. Kong, Y. Liu, D. Li, Overexpression of a maize dehydrin gene, ZmDHN2b,
521 in tobacco enhances tolerance to low temperature, Plant Growth Regul. 65 (2011) 109-118.

522

523 [28] A.E. Ochoa-Alfaro, M. Rodríguez-Kessler, M.B. Pérez-Morales, P. Delgado-Sánchez, C.L.
524 Cuevas-Velazquez, G. Gómez-Anduro, J.F. Jiménez-Bremont, Functional characterization of an
525 acidic SK 3 dehydrin isolated from an *Opuntia streptacantha* cDNA library. Planta 235 (2012)
526 565-578.

527

528 [29] H. Liu, C. Yu, H. Li, B. Ouyang, T. Wang, J. Zhang, X. Wang, Z. Ye, Overexpression of ShDHN,

529 a dehydrin gene from *Solanum habrochaites* enhances tolerance to multiple abiotic stresses in
530 tomato, *Plant Sci.* 231 (2015) 198-211.
531
532 [30] F. Bao, D. Du, Y. An, W. Yang, J. Wang, T. Cheng, Q. Zhang, Overexpression of *Prunus mume*
533 dehydrin genes in tobacco enhances tolerance to cold and drought, *Front. Plant Sci.* 8 (2017) 151.
534
535 [31] M. Hara, S. Terashima, T. Kuboi, Characterization and cryoprotective activity of
536 cold-responsive dehydrin from *Citrus unshiu*, *J. Plant Physiol.* 158 (2001) 1333-1339.
537
538 [32] L.A. Bravo, J. Gallardo, A. Navarrete, N. Olave, J. Martinez, M. Alberdi, T.J. Close, L.J.
539 Corcuera, Cryoprotective activity of a cold-induced dehydrin purified from barley, *Physiol. Plant.*
540 118 (2003) 262-269.
541
542 [33] S. Hughes, S.P. Graether, Cryoprotective mechanism of a small intrinsically disordered
543 dehydrin protein, *Protein Sci.* 20 (2011) 42-50.
544
545 [34] M. Drira, W. Saibi, F. Brini, A. Gargouri, K. Masmoudi, M. Hanin, The K-segments of the
546 wheat dehydrin DHN-5 are essential for the protection of lactate dehydrogenase and β -glucosidase
547 activities in vitro, *Mol. Biotech.* 54 (2013) 643-650.
548
549 [35] L.N. Rahman, F. McKay, M. Giuliani, A. Quirk, B.A. Moffatt, G. Harauz, J.R. Dutcher,
550 Interactions of *Thellungiella salsuginea* dehydrins TsDHN-1 and TsDHN-2 with membranes at cold
551 and ambient temperatures - Surface morphology and single-molecule force measurements show
552 phase separation, and reveal tertiary and quaternary associations, *Biochim. Biophys. Acta Biomembr.*

553 1828 (2013) 967-980.

554

555 [36] M. Hara, The multifunctionality of dehydrins: an overview. *Plant Signal. Behav.* 5 (2010)

556 503-508.

557

558 [37] A.A. Covarrubias, C.L. Cuevas-Velazquez, P.S. Romero-Pérez, D.F. Rendón-Luna, C.C. Chater,

559 Structural disorder in plant proteins: where plasticity meets sessility, *Cell. Mol. Life Sci.* 74 (2017)

560 3119-3147.

561

562 [38] S. Chakrabortee, R. Tripathi, M. Watson, G.S. Schierle, D.P. Kurniawan, C.F. Kaminski, M.J.

563 Wise, A. Tunnacliffe, Intrinsically disordered proteins as molecular shields, *Mol Biosyst.* 8 (2012)

564 210-219.

565

566 [39] J.L. Reyes, F. Campos, H.U.I. Wei, R. Arora, Y. Yang, D.T. Karlson, A.A. Covarrubias,

567 Functional dissection of hydrophilins during in vitro freeze protection, *Plant Cell Environ.* 31 (2008)

568 1781-1790.

569

570 [40] W. Yang, L. Zhang, H. Lv, H. Li, Y. Zhang, Y. Xu, J. Yu, The K-segments of wheat dehydrin

571 WZY2 are essential for its protective functions under temperature stress, *Front. Plant Sci.* 6 (2015)

572 406.

573

574 [41] M. Hara, Y. Shinoda, M. Kubo, D. Kashima, I. Takahashi, T. Kato, T. Horiike, T. Kuboi,

575 Biochemical characterization of the *Arabidopsis* KS-type dehydrin protein, whose gene expression is

576 constitutively abundant rather than stress dependent, *Acta Physiol. Plant.* 33 (2011) 2103-2116.

577

578 [42] M. Hara, S. Uchida, T. Murata, H. Wätzig, Efficient purification of cryoprotective dehydrin
579 protein from the radish (*Raphanus sativus*) taproot, Eur. Food Res. Technol. 239 (2014) 339-345.

580

581 [43] M. Hara, S. Monna, T. Murata, T. Nakano, S. Amano, M. Nachbar, H. Wätzig, The *Arabidopsis*
582 KS-type dehydrin recovers lactate dehydrogenase activity inhibited by copper with the contribution
583 of His residues, Plant Sci. 245 (2016) 135-142.

584

585 [44] C. Louis-Jeune, M.A. Andrade-Navarro, C. Perez-Iratxeta, Prediction of protein secondary
586 structure from circular dichroism using theoretically derived spectra, Proteins: Struct. Funct.
587 Bioinform. 80 (2012) 374-381.

588

589 [45] Z. Dosztányi, V. Csizmók, P. Tompa, I. Simon, The pairwise energy content estimated from
590 amino acid composition discriminates between folded and intrinsically unstructured proteins, J. Mol.
591 Biol. 347 (2005) 827-839.

592

593 [46] R. Linding, L.J. Jensen, F. Diella, P. Bork, T.J. Gibson and R.B. Russell, Protein disorder
594 prediction: implications for structural proteomics, Structure 11 (2003) 1453-1459.

595

596 [47] A. Lamiable, P. Thévenet, J. Rey, M. Vavrusa, P. Derreumaux, P. Tufféry, PEP-FOLD3: faster de
597 novo structure prediction for linear peptides in solution and in complex, Nucl. Acid. Res. 44 (2016)
598 W449-W454.

599

600 [48] P. Schuck, Size-distribution analysis of macromolecules by sedimentation velocity

601 ultracentrifugation and lamm equation modeling. *Biophys. J.* 78 (2000) 1606-1619.

602

603 [49] A.F. Monroy, Y. Castonguay, S. Laberge, F. Sarhan, L.P. Vezina, R.S. Dhindsa, A new
604 cold-induced alfalfa gene is associated with enhanced hardening at subzero temperature, *Plant*
605 *Physiol.* 102 (1993) 873-879.

606

607 [50] E.M. Rodriguez, J.T. Svensson, M. Malatrasi, D.W. Choi, T.J. Close, Barley Dhn13 encodes a
608 KS-type dehydrin with constitutive and stress responsive expression, *Theor. Appl. Genet.* 110 (2005)
609 852-858.

610

611 [51] T. Rorat, W.J. Grygorowicz, W. Irzykowski, P. Rey, Expression of KS-type dehydrins is
612 primarily regulated by factors related to organ type and leaf developmental stage during vegetative
613 growth, *Planta*, 218 (2004) 878-885.

614

615 [52] D. Kovacs, E. Kalmar, Z. Torok, P. Tompa, Chaperone activity of ERD10 and ERD14, two
616 disordered stress-related plant proteins, *Plant Physiol.* 147 (2008) 381–390.

617

618 [53] A.M. Ismail, A.E. Hall, T.J. Close, Purification and partial characterization of a dehydrin
619 involved in chilling tolerance during seedling emergence of cowpea, *Plant Physiol* 120 (1999)
620 237-244.

621

622 [54] J. Atkinson, M.W. Clarke, J.M. Warnica, K.F. Boddington, S.P. Graether, Structure of an
623 intrinsically disordered stress protein alone and bound to a membrane surface, *Biophys. J.* 111
624 (2016) 480-491.

625

626 [55] S. Eriksson, N. Eremina, A. Barth, J. Danielsson, P. Harryson, Membrane-induced folding of the
627 plant stress dehydrin Lti30, *Plant Physiol.* 171 (2016) 932-943.

628

629 [56] I.E. Hernández-Sánchez, D.M. Martynowicz, A.A. Rodríguez-Hernández, M.B. Pérez-Morales,
630 S.P. Graether, J.F. Jiménez-Bremont, A dehydrin-dehydrin interaction: the case of SK3 from *Opuntia*
631 *streptacantha*, *Front. Plant Sci.* 5 (2014) 520.

632

633 [57] I.E. Hernández-Sánchez, I. Maruri-López, S.P. Graether, J.F. Jiménez-Bremont, In vivo
634 evidence for homo- and heterodimeric interactions of *Arabidopsis thaliana* dehydrins AtCOR47,
635 AtERD10, and AtRAB18, *Sci. Rep.* 7 (2017) 1-13.

636

637 [58] R. Gautier, D. Douguet, B. Antony, G. Drin, HELIQUEST: a web server to screen sequences
638 with specific α -helical properties, *Bioinformatics* 24 (2008) 2101-2102.

639

640 [59] C.L. Cuevas-Velazquez, G. Saab-Rincón, J.L. Reyes, A.A. Covarrubias, The unstructured
641 N-terminal region of *Arabidopsis* group 4 late embryogenesis abundant (LEA) proteins is required
642 for folding and for chaperone-like activity under water deficit, *J. Biol. Chem.* 291 (2016)
643 10893-10903.

644

645 [60] I.S. Moreira, P.A. Fernandes, M.J. Ramos, Hot spots—A review of the protein–protein interface
646 determinant amino-acid residues, *Proteins: Struct. Funct. Bioinform.* 68 (2007) 803-812.

647

648 [61] A. Zhang, W. Qi, S.K. Singh, E.J. Fernandez, A new approach to explore the impact of

649 freeze-thaw cycling on protein structure: hydrogen/deuterium exchange mass spectrometry
650 (HX-MS), *Pharm. Res.* 28 (2011) 1179-1193.

651

652 [62] P. Tompa, P. Csermely, The role of structural disorder in the function of RNA and protein
653 chaperones, *FASEB J.* 18 (2004) 1169-1175.

654

655 [63] C.L. Cuevas-Velazquez, D.F. Rendón-Luna, A.A. Covarrubias, Dissecting the cryoprotection
656 mechanisms for dehydrins, *Front. Plant Sci.* 5 (2014) 583.

657

658

659 **Figure legends**

660

661 **Fig. 1.** AtHIRD11 and AtHIRD11 Φ /T used in this study. Amino acid sequences of AtHIRD11 (A)
662 and AtHIRD11 Φ /T (B). K-segment, mutated K-segment, and S-segments are shadowed. Underlines
663 indicate hydrophobic amino acids in AtHIRD11, and Ts in AtHIRD11 Φ /T correspond to the
664 hydrophobic amino acids in AtHIRD11. (C, D) AtHIRD11, AtHIRD11 Φ /T, FITC-AtHIRD11, and
665 FITC-AtHIRD11 Φ /T were analyzed by SDS-PAGE. (C) AtHIRD11 and AtHIRD11 Φ /T were
666 visualized by Coomassie blue staining. Protein amounts were 2 μ g (lane 1), 1 μ g (lane 2), and 0.4 μ g
667 (lane 3). (D) FITC-AtHIRD11 and FITC-AtHIRD11 Φ /T were detected by a fluorescence imaging
668 system. Proteins were loaded at 5 ng (lane 1), 0.5 ng (lane 2), and 0.1 ng (lane 3). Open and closed
669 arrowheads represent AtHIRD11 (or FITC-AtHIRD11) and AtHIRD11 Φ /T (or FITC-AtHIRD11 Φ /T).
670 Adjustments of brightness and contrast were applied to every pixel in the original images.

671

672 **Fig. 2.** Cryoprotective activities of AtHIRD11 and AtHIRD11 Φ /T. Inhibition of cryoinactivation (A),

673 cryodenaturation (B), and cryoaggregation (C) is shown as PD₅₀ values. The concentration of LDH
674 as a monomer was 0.14 μM. Columns and bars represent means ± SD (four experiments). Because
675 the PD₅₀ values of AtHIRD11Φ/T were more than 60 μM (A) and 35 μM (B and C), the tops of the
676 columns appear as broken.

677

678 **Fig. 3.** Cryoprotective activities of AtHIRD11 segments. (A) Corresponding sites for NK1-6 and
679 Kseg are shown. Hydrophobic amino acids are underlined. (B) Inhibition of cryoinactivation,
680 cryodenaturation, and cryoaggregation is shown as PD₅₀ values. The concentration of LDH as a
681 monomer was 0.14 μM. Columns and bars represent means ± SD (four experiments). Asterisks
682 indicate significant differences ($p < 0.05$) from NK1. When the PD₅₀ values were more than 300 μM,
683 the tops of the columns appear as broken. In these cases, the asterisks are not labeled.

684

685 **Fig. 4.** Secondary structures of AtHIRD11 and AtHIRD11Φ/T. (A) Prediction of disorder by using
686 IUPred (<https://iupred2a.elte.hu/>) [45]. AtHIRD11 and AtHIRD11Φ/T are shown in solid and broken
687 lines, respectively. The locations of segments are represented. (B) The CD spectra for AtHIRD11 and
688 AtHIRD11Φ/T. SDS was added at concentrations of 0 mM (gray broken lines), 0.1 mM (gray solid
689 lines), 1 mM (black broken lines), and 10 mM (black solid lines). The negative peaks corresponding
690 to random structures are indicated by arrowheads. (C) Secondary structure contents of AtHIRD11
691 and AtHIRD11Φ/T. Contents of alpha-helix (α) and beta-strand (β) were assessed from the data in B
692 by using K2D3 software (<http://cbdm-01.zdv.uni-mainz.de/~andrade/k2d3/>) [44]. Asterisks indicate
693 significant differences ($p < 0.05$) from 0 mM SDS.

694

695 **Fig. 5.** Secondary structures of AtHIRD11 segments. (A) The CD spectra of the segments. SDS was
696 added at concentrations of 0 mM (gray broken lines), 0.1 mM (gray solid lines), 1 mM (black broken

697 lines), and 10 mM (black solid lines). The negative peaks corresponding to random structures are
 698 indicated by arrowheads. (B) Secondary structure contents of segments. Contents of alpha-helix (α)
 699 and beta-strand (β) were assessed from the data in A by using K2D3 software
 700 (<http://cbdm-01.zdv.uni-mainz.de/~andrade/k2d3/>) [44]. Asterisks indicate significant differences (p
 701 < 0.05) from 0 mM SDS.

702

703

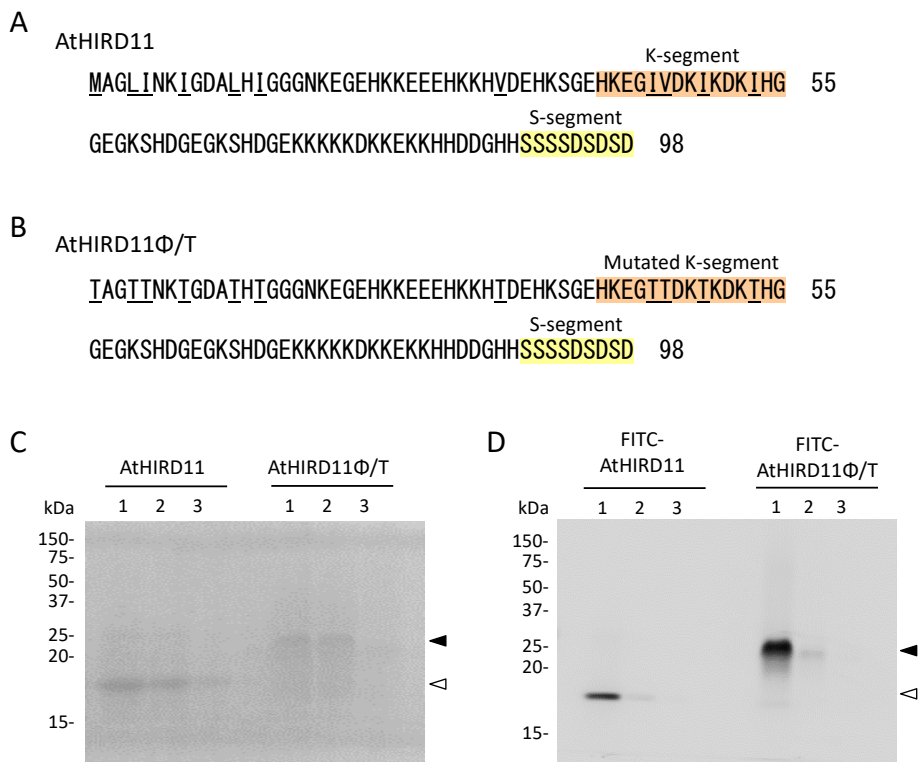


Fig. 1 Yokoyama et al.

704

705

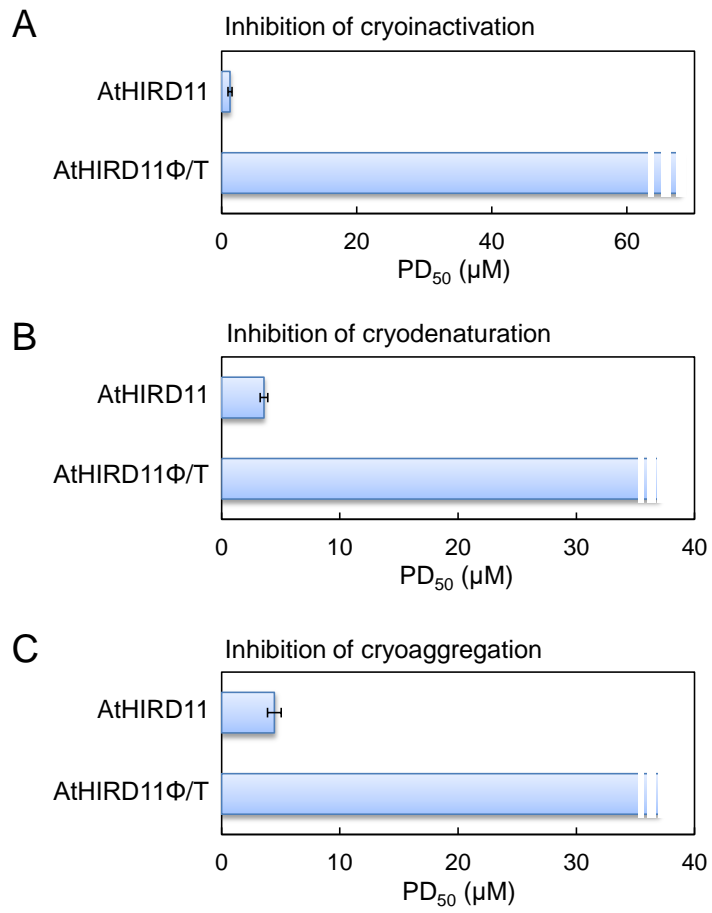


Fig. 2 Yokoyama et al.

706

707

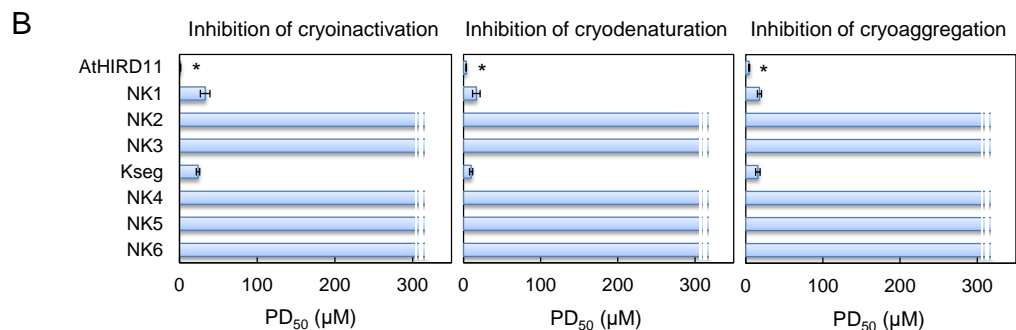
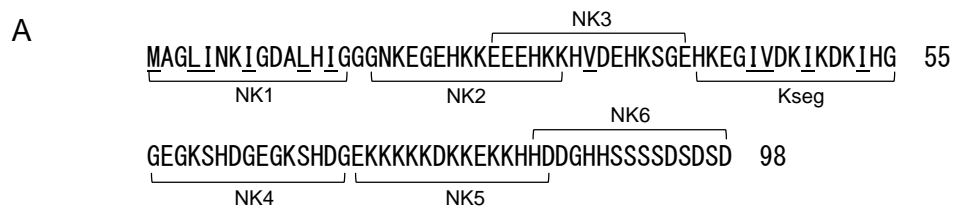


Fig. 3 Yokoyama et al.

708

709

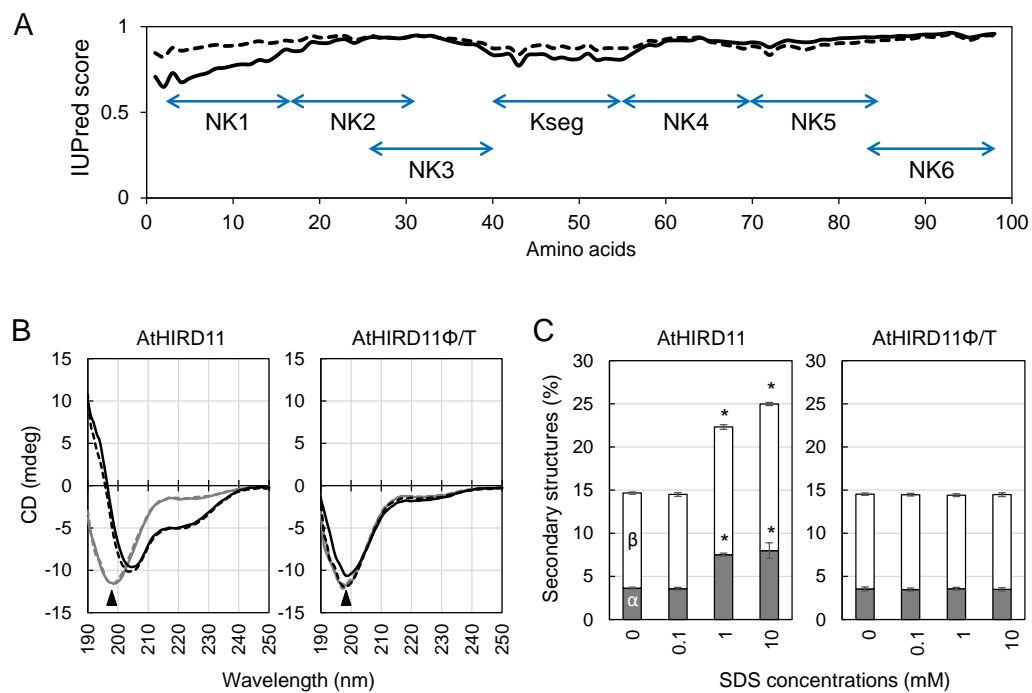


Fig. 4 Yokoyama et al.

710

711

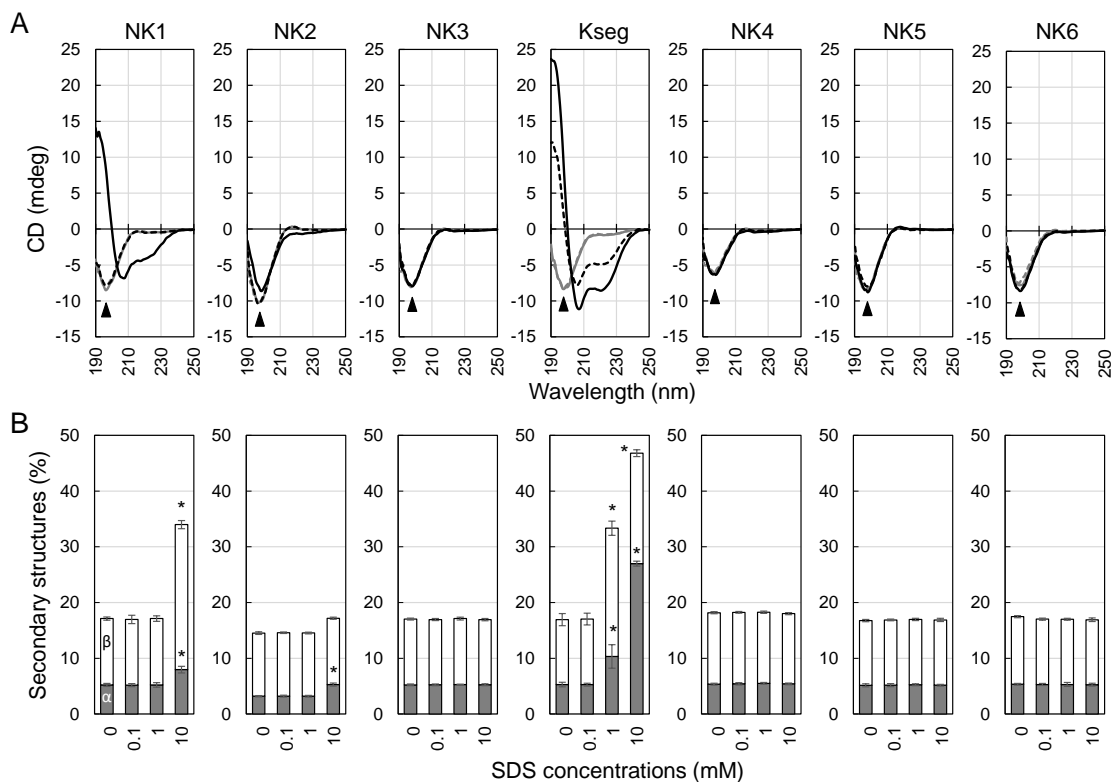


Fig. 5 Yokoyama et al.

712

713

714

Table 1

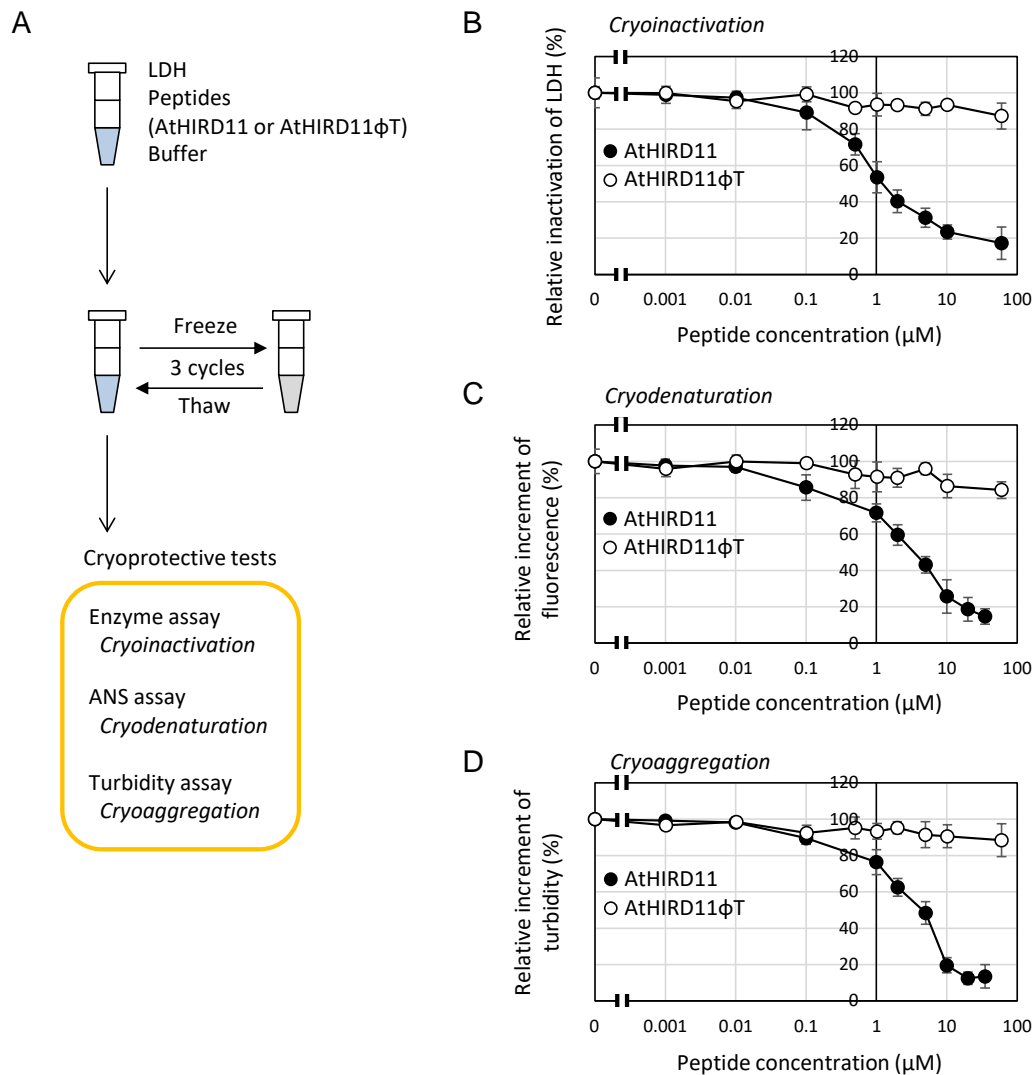
Molecular weights of peptides determined by analytical ultracentrifugation.

	Molecular weight		Calculated molecular weight
	#1	#2	
FITC-AtHIRD11	14,000	14,200	11,298
FITC-AtHIRD11Φ/T	14,300	13,700	11,236

Experiments were conducted twice (#1 and #2).

715

716



Supplementary Fig. 1. Cryoprotective tests for lactate dehydrogenase (LDH). (A) An assay scheme. Samples containing LDH, peptides (AtHIRD11 or AtHIRD11 Φ T), and buffer were treated with three freeze-and-thaw cycles. Enzyme activity (cryoinactivation), 8-anilino-1-naphthalene sulfonate (ANS) fluorescence (ex 350 nm, em 470 nm) (cryodenaturation), and turbidity (cryoaggregation) were then determined. Relative cryoinactivation of LDH (B), relative fluorescence intensity (C), and relative turbidity (D) are shown. Values and bars represent means \pm SD (four experiments).

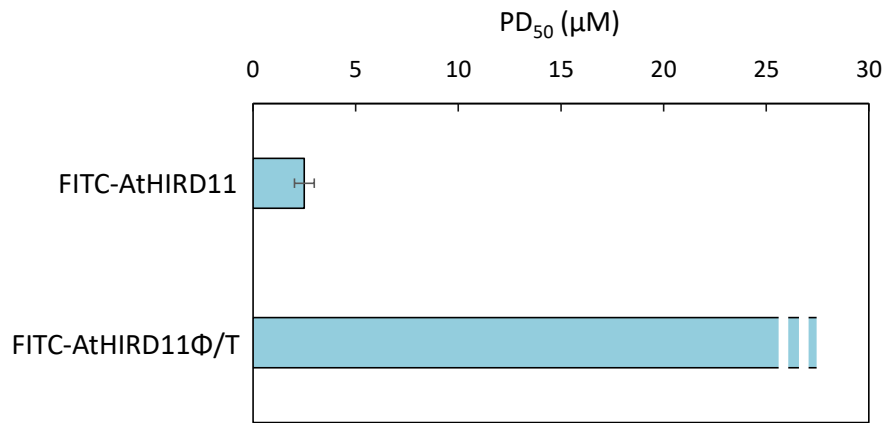
Title: Cryoprotective activity of *Arabidopsis* KS-type dehydrin depends on the hydrophobic amino acids of two active segments.

Authors: Yokoyama T, Ohkubo T, Kamiya K, Hara M*

*hara.masakazu@shizuoka.ac.jp

717

718



Supplementary Fig. 2. Inhibition of cryoinactivation of lactate dehydrogenase (LDH) by fluorescein isothiocyanate (FITC)-labeled proteins (AtHIRD11 and AtHIRD11Φ/T). The PD₅₀ values and bars represent means ± SD (four experiments).

Title: Cryoprotective activity of *Arabidopsis* KS-type dehydrin depends on the hydrophobic amino acids of two active segments.

Authors: Yokoyama T, Ohkubo T, Kamiya K, Hara M*

*hara.masakazu@shizuoka.ac.jp

719

720

AtHIRD11

Disordered by Loops/coils definition

>none_LOOPS 10-98

maglinkigD **ALHIGGGNKE GEHKKEEEHK KHVDEHKSGE HKEGIVDKIK DKIHGGEGKS HDGEGKSHDG EKKKKKDKKE KKHDDGHHS SSSDSDS**

Disordered by Hot-loops definition

>none_HOTLOOPS 1-24, 29-98

MAGLINKIGD ALHIGGGNKE GEHK^{keee}HK KHVDEHKSGE HKEGIVDKIK DKIHGGEGKS HDGEGKSHDG EKKKKKDKKE KKHDDGHHS SSSDSDS

Disordered by Remark-465 definition

>none_REM465 19-40, 55-98

maglinkigd alhigggn**KE GEHKKEEEHK KHVDEHKSGE** hkegivdkik dkih**GGEGKS HDGEGKSHDG EKKKKKDKKE KKHDDGHHS SSSDS**

AtHIRD11Φ/T

Disordered by Loops/coils definition

>none_LOOPS 1-98

TAGTTNKTGD ATHTGGGNKE GEHKKEEEHK KHTDEHKSGE HKEGTTDKTK DKTHGGEGKS HDGEGKSHDG EKKKKKDKKE KKHDDGHHS SSSDSDS

Disordered by Hot-loops definition

>none_HOTLOOPS 1-98

TAGTTNKTGD ATHTGGGNKE GEHKKEEEHK KHTDEHKSGE HKEGTTDKTK DKTHGGEGKS HDGEGKSHDG EKKKKKDKKE KKHDDGHHS SSSDSDS

Disordered by Remark-465 definition

>none_REM465 1-98

TAGTTNKTGD ATHTGGGNKE GEHKKEEEHK KHTDEHKSGE HKEGTTDKTK DKTHGGEGKS HDGEGKSHDG EKKKKKDKKE KKHDDGHHS SSSDSDS

Supplementary Fig. 3. Disordered regions of AtHIRD11 and AtHIRD11Φ/T were predicted by DisEMBL Intrinsic Protein Disorder Prediction 1.5 (<http://dis.embl.de/>). Three types of predictions were provided. Disordered sequences are shown in bold.

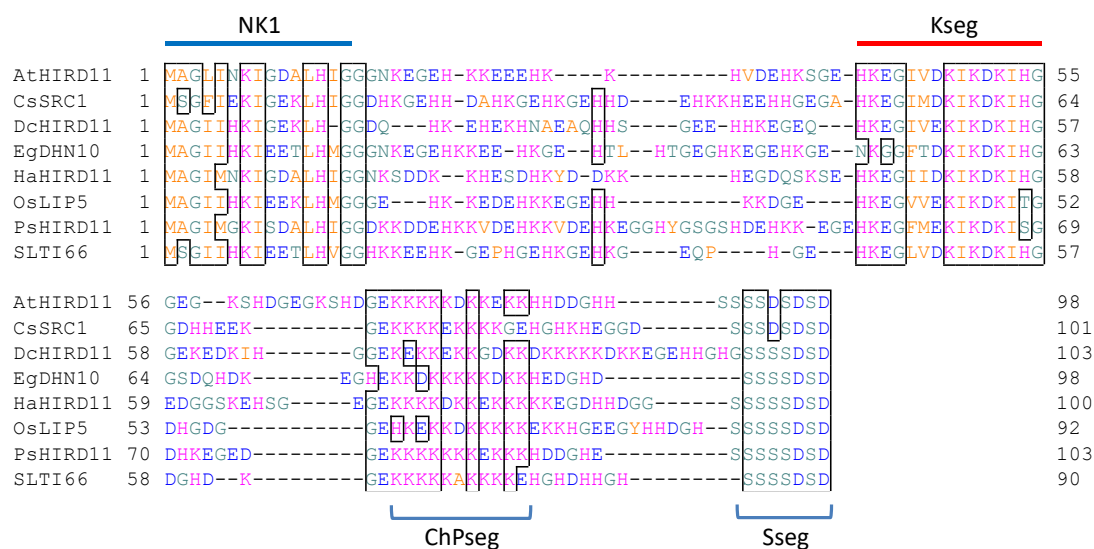
Title: Cryoprotective activity of *Arabidopsis* KS-type dehydrin depends on the hydrophobic amino acids of two active segments.

Authors: Yokoyama T, Ohkubo T, Kamiya K, Hara M*

*hara.masakazu@shizuoka.ac.jp

721

722



Supplementary Fig. 4. AtHIRD11 and related KS-type dehydrins. Amino acid sequences were aligned by Genetyx 6.0. AtHIRD11, *Arabidopsis thaliana* (At1g54410); CsSRC1, *Cucumis sativus* (XP_011652200); DcHIRD11, *Dendrobium catenatum* (XP_020686886); EgDHN10, *Eucalyptus globulus* (AER27689); HaHIRD11, *Helianthus annuus* (XP_021994491); OsLIP5, *Oryza sativa* (BAA24979); PsHIRD11, *Papaver somniferum* (XP_026426999); and SLTI66, *Glycine max* (ABO70349). Hydrophobic residues, positively charged residues, negatively charged residues, and others are shown in orange, magenta, blue, and green, respectively. Sites of NK1, K-segment (Kseg), ChP-segment (ChPseg), and S-segment (Sseg) are indicated.

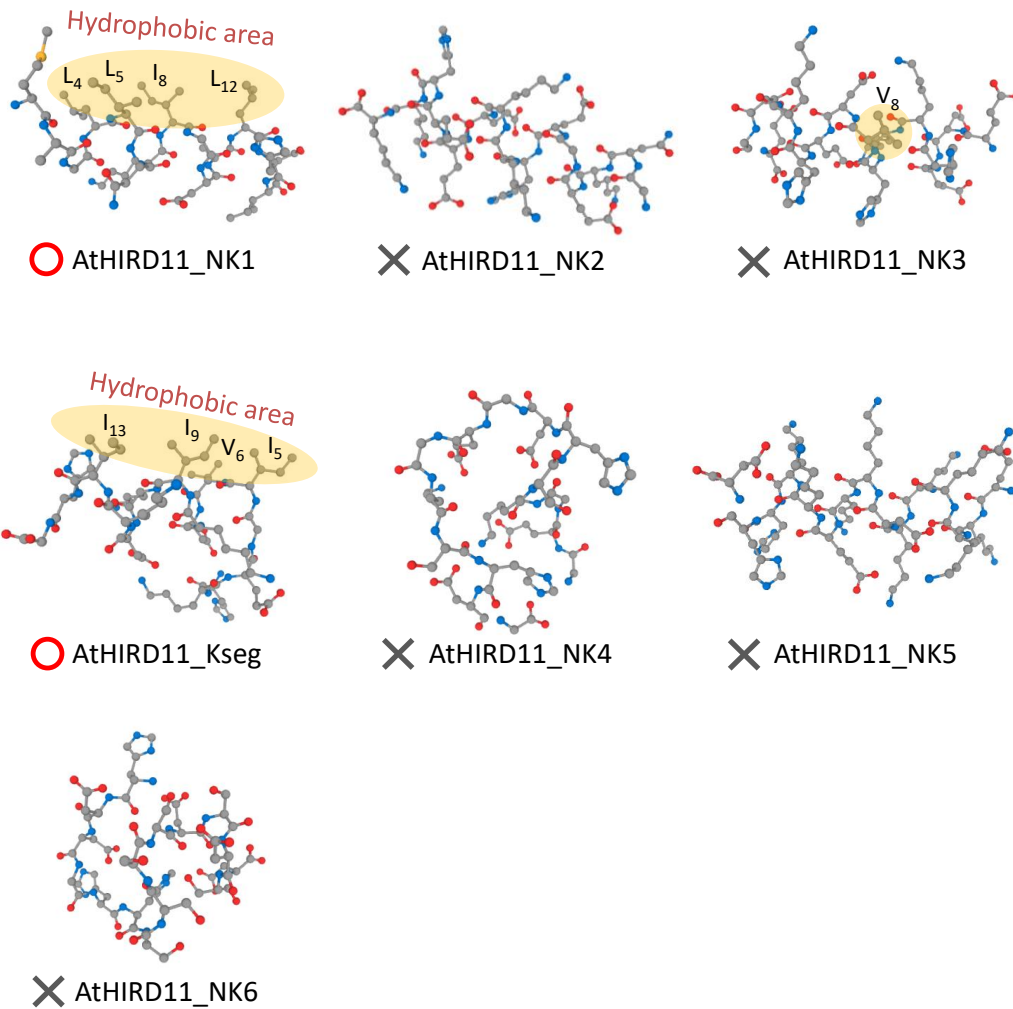
Title: Cryoprotective activity of *Arabidopsis* KS-type dehydrin depends on the hydrophobic amino acids of two active segments.

Authors: Yokoyama T, Ohkubo T, Kamiya K, Hara M*

*hara.masakazu@shizuoka.ac.jp

723

724



Supplementary Fig. 6. Tertiary structures were predicted by using PEP-FOLD3 software (<https://mobylye.rpbs.univ-paris-diderot.fr/cgi-bin/portal.py#forms::PEP-FOLD3>). Seven segments were analyzed. Hydrophobic areas are shown in yellow. Hydrophobic amino acids related to the hydrophobic areas are shown. Red circles and black Xs represent peptides having potent and little cryoprotective activities, respectively.

Title: Cryoprotective activity of *Arabidopsis* KS-type dehydrin depends on the hydrophobic amino acids of two active segments.

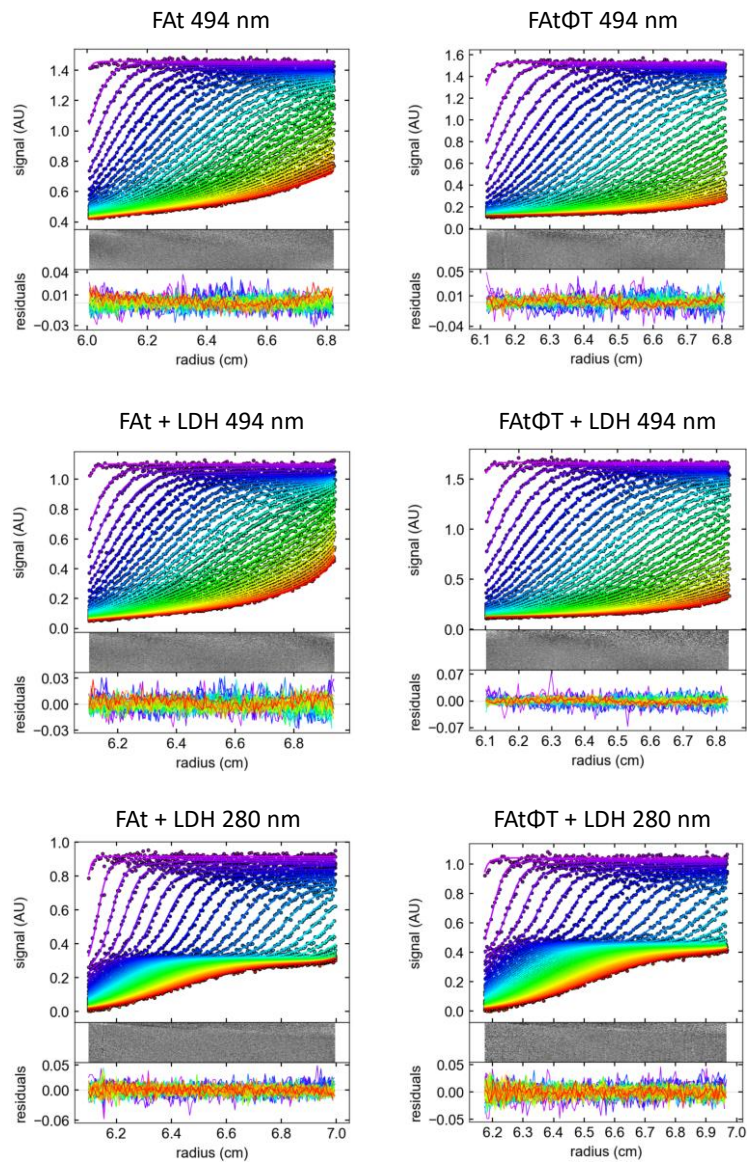
Authors: Yokoyama T, Ohkubo T, Kamiya K, Hara M*

*hara.masakazu@shizuoka.ac.jp

727

728

A



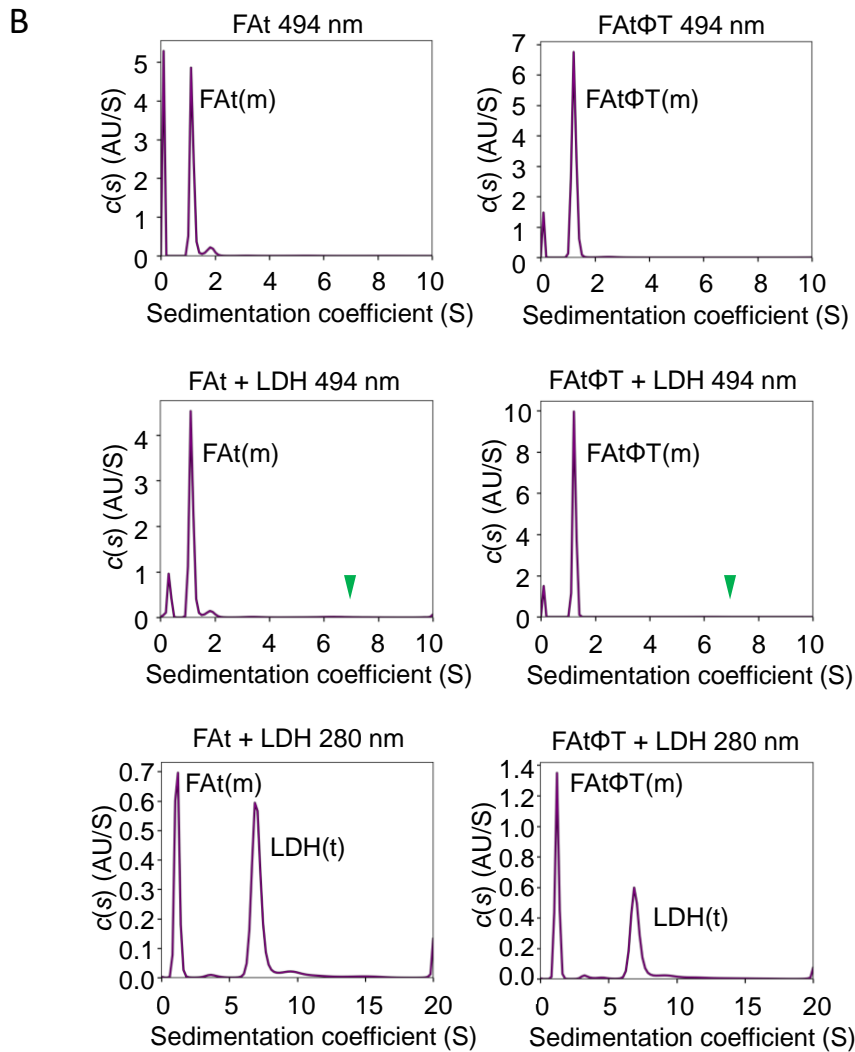
Supplementary Fig. 7. (continued)

Title: Cryoprotective activity of *Arabidopsis* KS-type dehydrin depends on the hydrophobic amino acids of two active segments.

Authors: Yokoyama T, Ohkubo T, Kamiya K, Hara M*
*hara.masakazu@shizuoka.ac.jp

729

730



Supplementary Fig. 7. Ultracentrifuge analysis. Samples containing lactate dehydrogenase (LDH) and fluorescein isothiocyanate (FITC)-labeled proteins (FITC-AtHIRD11 and FITC-AtHIRD11 Φ /T) were centrifuged at 50,000 rpm by using Optima XL-I analytical ultracentrifuge (Beckman-Coulter). The moving boundaries and the residuals between raw and theoretically fitted data points were obtained (A). Subsequently, the distribution of sedimentation coefficients was calculated by the $c(s)$ method in SEDFIT (B). Peaks corresponding to monomer (m) and tetramer (t) were detected. FAt and FAt Φ T represent FITC-AtHIRD11 and FITC-AtHIRD11 Φ /T, respectively. Detection wavelengths (280 nm and 494 nm) are shown. Arrowheads indicate the positions of LDH. The concentrations of FITC-labeled proteins and LDH were 30 μ M and 20 μ M, respectively.

Title: Cryoprotective activity of *Arabidopsis* KS-type dehydrin depends on the hydrophobic amino acids of two active segments.

Authors: Yokoyama T, Ohkubo T, Kamiya K, Hara M*

*hara.masakazu@shizuoka.ac.jp